Spectrum of Engineering Sciences
ISSN (e) 3007-3138 (p) 3007-312X Volume 4, Issue 5, 2026

INTERACTION OF STRESS CORROSION CRACKING WITH LOW CYCLIC FATIGUE USING TIME-INTEGRATION FRAMEWORK

Syed Muhammad Talha Hassan Shah[1], Rehmat Bashir[*2], Muhammad Bilal Hussain[3], Ali Soban[4], Muhammad Asghar[5]

[1,*2,3,4,5]*Department of Mechanical Engineering, University of Engineering and Technology Lahore 54890, Pakistan*

[*2]rehmatbashir@uet.edu.pk

DOI: https://doi.org/10.5281/zenodo.20337925

Keywords

Stress corrosion cracking; Low cyclic fatigue; Overall crack growth rate

Article History

Received: 22 March 2026

Accepted: 01 May 2026

Published: 22 May 2026

Corresponding Author: *

Rehmat Bashir

Abstract

The numerical results of the stress corrosion cracking (SCC) have been different from those of experimental results. Recent research indicate that numerical results of the SCC are compatible if the Cyclic load (Fatigue) is considered while simulating the SCC crack, however, the mechanism to combine the fatigue and SCC has gained much attention and has been a hot area of research as SCC and fatigue crack follow different mechanism during propagation, earlier demands the stress intensity factor (K) to be constant while later needs change in stress intensity factor (Δ K). In this research, a mechanism has been developed to combine SCC and Fatigue crack propagation (referred as overall crack propagation, da/dN_0) based on film rupture, Paris regime, and Time-Integration Models. At the end the numerical results of the overall crack growth rate have been compared with results available in literature based on linear superposition methods. It has been observed that the da/dN_0 calculated based on Time-Integration Models generates results closer to the experimental values.

1. INTRODUCTION

The material like austenitic steel- 304 used in structures are famous for their strengths against high loads and corrosive environment which makes them suitable for the locations where structural integrity is of high concern e.g. in nuclear power plants (NPPs). It's too costly to bear any failure in these industries[1]. Therefore, before going in service this steel should be tested and designed for the required load conditions to avoid any failure. Excessive studies on this area reveals that there are two modes of material degradation, i.e. fatigue crack and stress corrosion cracking (SCC)[2]. **SCC** is generally environmentally assisted cracking under sustained or slowly varying tensile stress considering constant stress intensity factor (K) in susceptible material/environment system[3], while **fatigue** is cyclic loading and occurs due to the variation in the stress intensity factor (Δ K)[4] and can be categorized as low cyclic fatigue (LCF) and high cyclic fatigue (HCF). High cycle fatigue (HCF) typically involves a large number of loading cycles before failure occurs under an applied load. This suggests that the applied load is not high enough to cause rapid cracking, and thus, it is not considered a failure regime in the conventional sense, while the **low cyclic fatigue** (LCF) has

low cycle counts and higher plastic strain amplitudes, making cyclic plasticity an important contributor to damage accumulation and crack growth behaviour[5], [6].

Extensive literature exists on crack propagation under SCC and LCF investigated independently[7], [8], [9], [10]. such as: Xue et al. [11]investigated the mechanical driving forces governing SCC crack growth rate in dissimilar metal weld joint (DMWJ). Their work shows that the crack tip mechanical state is highly non-uniform and strongly influenced by microstructural heterogeneity and residual stresses. Consequently, accurate SCC crack growth prediction requires quantitative, locally resolved driving force characterization at the microstructural scale. Similarly, T. Chu et al. investigated the behaviour of SCC in weld metal (WM) and heat effected zone (HAZ) observed more prominent crack propagation in HAZ [12]than Y. Zhang et al. [13]examined the impact of varying relative humidity in the presence of $MgCl_2$, Meisnar et al.[14] assessed impact of temperature. while Du et al. studied the impact of temperature along dissolved oxygen on SCC crack propagation.

Similarly, for LCF, Elber introduced the concept of crack closure which links the fatigue crack growth behaviour to stress ratio (R) variation[15]. Paris and Erdogan proposed the following relation for fatigue crack propagation[16],

$$\frac{da}{dN} = C(\Delta K)^m$$

where da/dN is the crack growth per cycle, ΔK is the stress intensity factor range, and C and m are material constants. Various developments in Paris Law results in models like Forman equation and Walker equation. Kebir *et al.* developed a parametric fatigue crack growth (FCG) model and implemented it in MATLAB, using Paris, Walker, and Forman equations to investigate the influences of stress intensity factor range (ΔK), stress ratio (R), and fracture toughness on fatigue crack growth behaviour[17].

None of the above-mentioned models considered the effect of SCC on fatigue crack propagation and vice versa. Both the loads act simultaneously on the same crack. Very few studies have explicitly accounted for the simultaneous action of SCC and LCF at the crack tip. W.Y. Maeng *et al.* investigated both the individual and combined effects of SCC and LCF on crack growth behaviour in Alloy 600 under high-temperature, pressurized water conditions, and concluded that the combined SCC and LCF loading produced the highest CGR[18]. S. Mohanty et al. discussed the literature on corrosion fatigue and SCC interaction on LWR colling system components[19]. M. Knop et al. studied the effect of cycle frequency on CGR under combined SCC and LCF[20]. Based on his observation he proposed a mechanistic model in which the CGR is represented as a sigmoidal function of cycle rise time. This model accounts explicitly for the interaction between electrochemical processes at the crack tip and cyclic plasticity. Bashir *et al.* investigated crack growth behaviour in SS 304 under combined SCC and LCF loading using the extended finite element method (XFEM)[21]. The crack growth rates were evaluated using a linear superposition approach, and it was concluded that, once a crack is initiated, SCC becomes the dominant contributor to subsequent crack propagation. Huang *et al.* demonstrated that prior LCF could modify microstructure and residual stress in CrNiMoV steel, leading to reduced SCC susceptibility[22]. Their findings highlight that LCF does not necessarily accelerate SCC but can alter crack paths and local driving forces through microstructural evolution. This supports the need to consider mechanistic SCC–LCF interaction models rather than simple superposition approaches.

In our study, time-integration framework is adopted to model the combined impact of SCC and LCF on CGR. In this framework, total CGR per cycle is computed by adding the cycle dependent fatigue crack advance and time dependent SCC growth over the cycle duration. Fatigue crack growth follows Paris' law:

$$\frac{da}{dN_{\text{LCF}}} = C\,(\Delta K)^m$$

SCC crack growth is expressed as film rupture re-passivation model.

$$\frac{da}{dt}_{\text{SCC}} = \left[\frac{M}{pZF} Q_f \frac{\dot{\varepsilon}_{\text{tip}}}{\dot{\varepsilon}_{\text{f}}}\right]$$

Where M, p, Z, F, Q_f are constants related to the film rupture mechanism and material/environmental factors, $\dot{\varepsilon}_{\text{tip}}$ is strain rate at the crack tip and $\dot{\varepsilon}_{\text{f}}$ is fracture strain rate. This equation gives crack growth per unit time, typically in mm/s.

In the time-integration model, convert SCC per unit time to per-cycle growth by integrating over the duration of the cycle t_{cycle}.

$$\Delta a_{\text{SCC, cycle}} = \int_0^{t_{\text{cycle}}} \frac{da}{dt}_{\text{SCC}}\, dt$$

If the crack tip strain rate is approximately constant within a cycle, this simplifies to:

$$\Delta a_{\text{SCC, cycle}} \approx \frac{da}{dt}_{\text{SCC}} \cdot t_{\text{cycle}}$$

Then, the total crack growth per cycle becomes:

$$\frac{da}{dN_{\text{total}}} = \Delta a_{\text{SCC, cycle}} + \frac{da}{dN_{\text{LCF}}}$$

2. Material and Method

2.1. Material

The material used in this research is austenitic Steel-304(SS-304), as austenitic stainless steels are extensively used in aggressive service environments such as light water reactors (LWRs) due to their favourable mechanical and corrosion resistance properties. Low-carbon SS-304 is utilized in this research because of its widespread application in structural and pressure-retaining components[23], [24]. The chemical and mechanical properties of the material are listed in Tables 1 and 2.

Table 1:Chemical composition of the used stainless steel (wt%).

Steel	C	Si	Mn	P	S	Cr	N	Ni
304	0.08	0.75	2.00	0.045	0.03	18-20	0.1	8-10

Table 2: Elastic properties of the SS-304 used.

Material	Elastic modulus (GPa)	Maximum principle stress (MPa)	Poisson's ratio	Elongation (%)
SS-304	210	550	0.32	40

2.2. Methodology

A two-dimensional rectangular plate with dimensions of 100 mm × 50 mm is considered. A crack of 25 mm length is introduced using the extended finite element method (XFEM), as illustrated in Figure 1(b), along with the applied boundary conditions and loading. The analysis is performed under plane stress conditions. Crack initiation and propagation are modelled using the XFEM, which enables discontinuities to be represented independently of the mesh and eliminates the need for remeshing during crack growth. The model is discretized using four-node reduced integration elements. A finer mesh is employed in the vicinity of the crack tip to accurately capture stress concentration effects, while a relatively coarser mesh is used away from the crack region to improve computational efficiency. Boundary conditions are applied to restrict rigid body motion. The bottom edge of the plate is constrained in the vertical direction, and horizontal displacement is restricted at a reference point to prevent lateral movement. A uniform tensile stress of 200 MPa, 210MPa and 215MPa are applied on the top surface of the plate, as illustrated in Figure X. The load is applied gradually during a static analysis step.

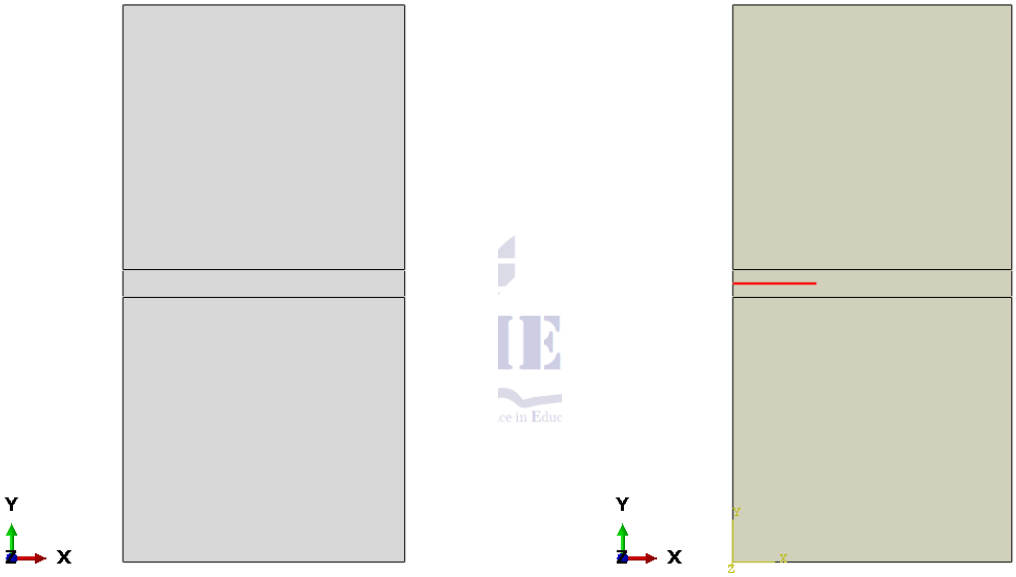

(a) 2D Plate (b) 2D Plate with Crack

Figure 1. The plate used for the XFEM analysis

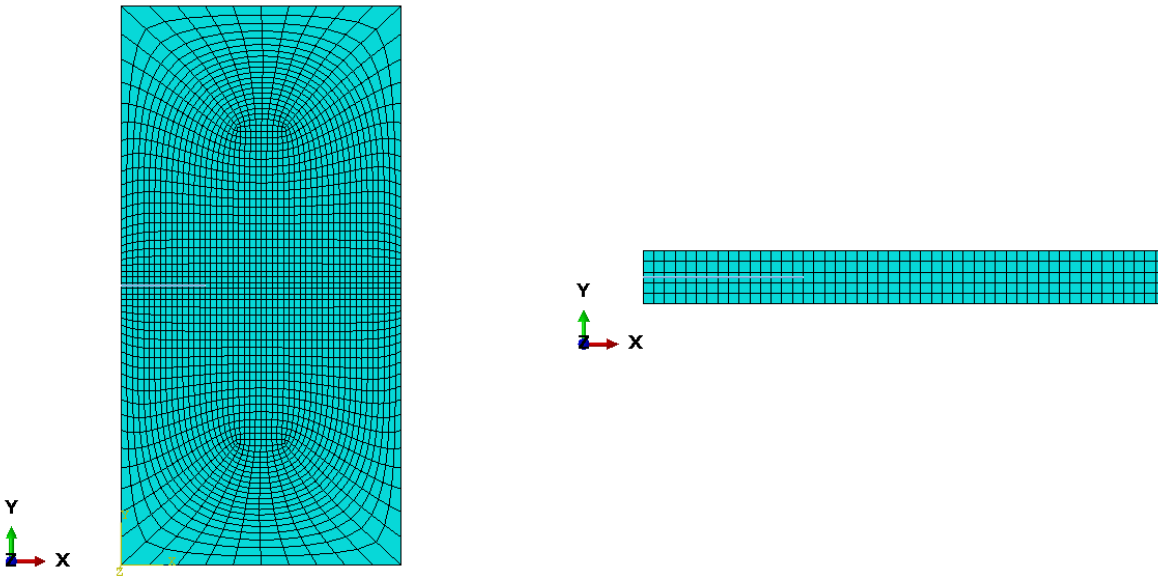

(a) (b)

lobal Mesh ocal Mesh

Figure 2. Mesh of the XFEM analysis

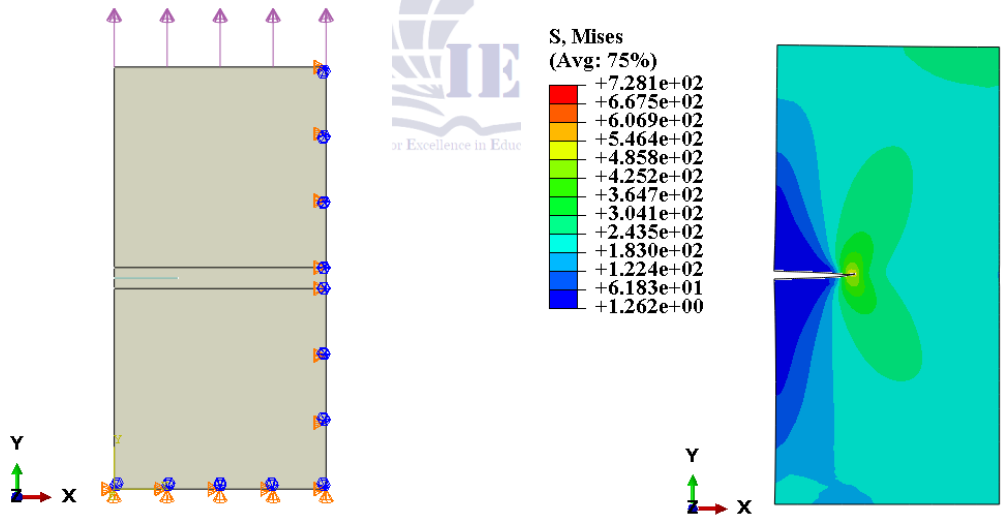

(a) (b)

oundary Conditions on Mises

Figure 3. Boundary conditions and crack movement

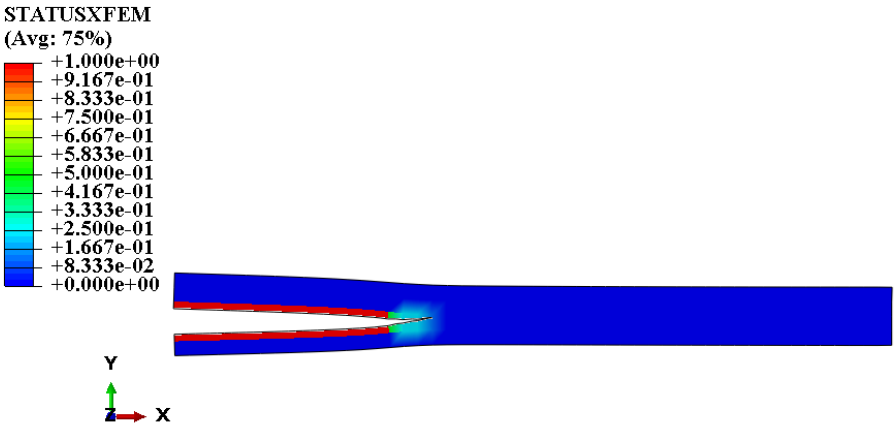

Figure 4. Status XFEM

3. Results and Discussions

Figure 5 presents the normal plastic strain distribution as a function of distance from the crack tip for different applied stress levels. The maximum strain occurs at the crack tip due to stress concentration and decreases sharply with distance, indicating localized plastic deformation. Increasing applied stress enhances both the magnitude and extent of the plastic zone. Such elevated crack-tip plasticity is expected to significantly influence stress corrosion cracking behaviour by promoting localized damage and accelerating crack growth.

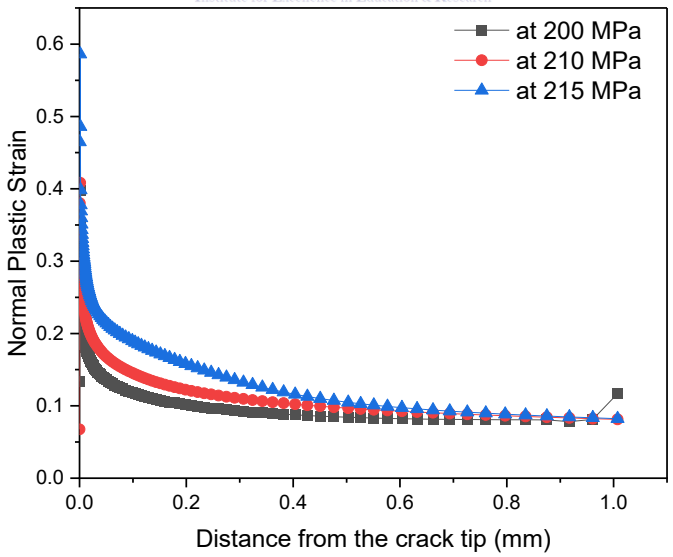

Figure 5. Normal strain vs. distance from crack tip at different

Figure 6 shows the variation of SCC crack growth rate with distance from the crack tip at applied stresses of 200 MPa, 210 MPa, and 215 MPa. The maximum crack growth rate occurs at the crack

tip, where stress concentration and plastic strain are highest, and decreases rapidly with increasing distance. An increase in applied stress significantly elevates the crack growth rate, indicating enhanced crack-tip driving force. The observed trend suggests a strong coupling between mechanical loading, localized plastic deformation, and corrosion-assisted crack propagation.

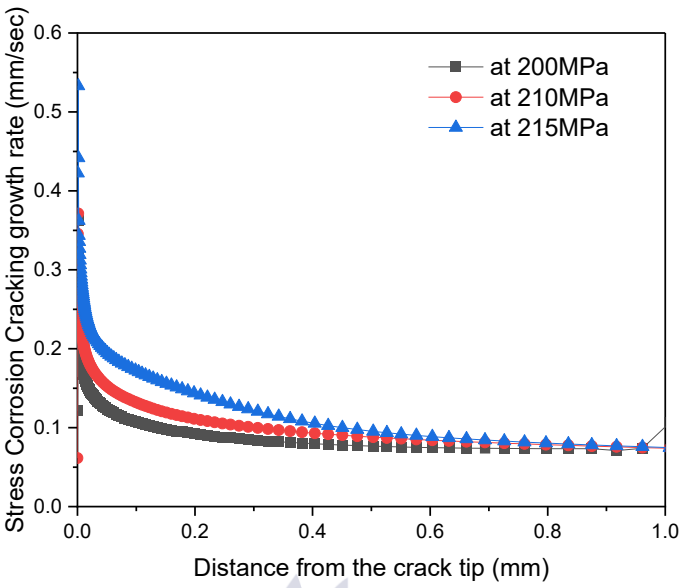

Figure 6. SCC crack growth rate vs. distance from crack tip

Bashir et al.[25] has defined the mechanism to convert the SCC from mm/sec to mm/sec, which has been applied here. **Figure 7** shows the variation of SCC crack growth rate (mm/cycle) with distance from the crack tip at applied stresses of 200, 210, and 215 MPa. The growth rate reaches its maximum at the crack tip distanceindicating that crack propagation is strongly localized in the near-tip region. A clear increase in crack growth rate is observed with increasing applied stress, reflecting the enhanced crack-tip driving force under higher loading. These results suggest that SCC propagation is primarily controlled by local stress intensity and deformation conditions at the crack tip.

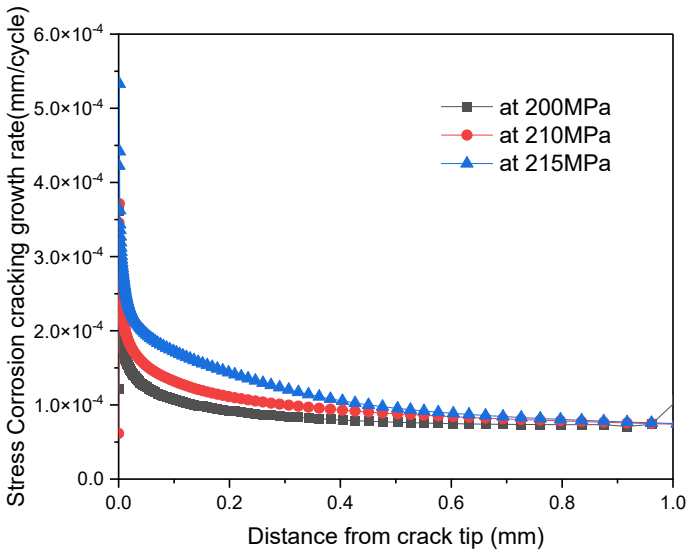

Figure 7. SCC crack growth rate (mm/cycle) vs. distance from crack tip

Figure 8 shows the variation of low cycle fatigue (LCF) crack growth rate (mm/cycle) with distance from the crack tip at applied stresses of 200, 210, and 215 MPa. Similar to the SCC response, the crack growth rate is highest at the crack tip and decreases rapidly with increasing distance, indicating strong localization of cyclic plastic deformation in the near-tip region. Increasing the applied stress results in a noticeable rise in crack growth rate, demonstrating the sensitivity of fatigue crack propagation to stress amplitude. These results confirm that LCF crack growth is primarily governed by crack-tip stress–strain conditions and the accumulation of cyclic plastic damage.

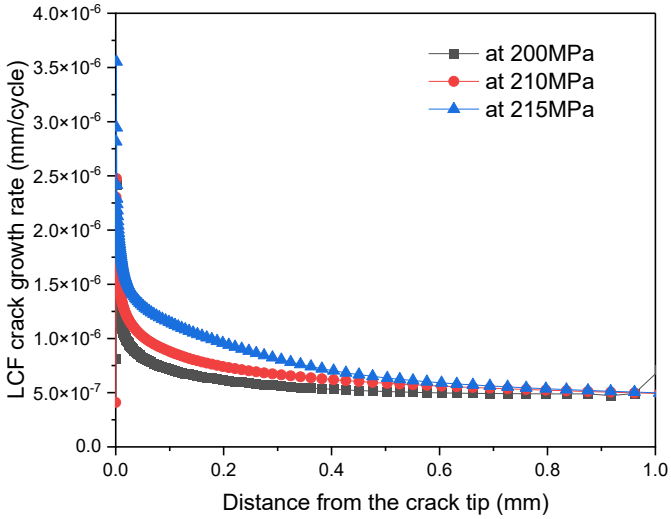

Figure 8. LCF crack growth rate (mm/cycle) vs. distance from crack tip

Figure 9 presents the variation of the overall crack growth rate (mm/cycle) with distance from the crack tip under applied stresses of 200, 210, and 215 MPa. The crack growth rate attains its maximum at the crack tip and decreases progressively with increasing distance, indicating that crack propagation is predominantly governed by near-tip conditions. A systematic increase in growth rate is observed with increasing applied stress, reflecting the combined influence of enhanced stress intensity and localized plastic deformation. The observed trend suggests that the overall crack propagation behavior results from the coupled interaction of cyclic fatigue damage and corrosion-assisted mechanisms, both of which are strongly concentrated in the crack-tip region.

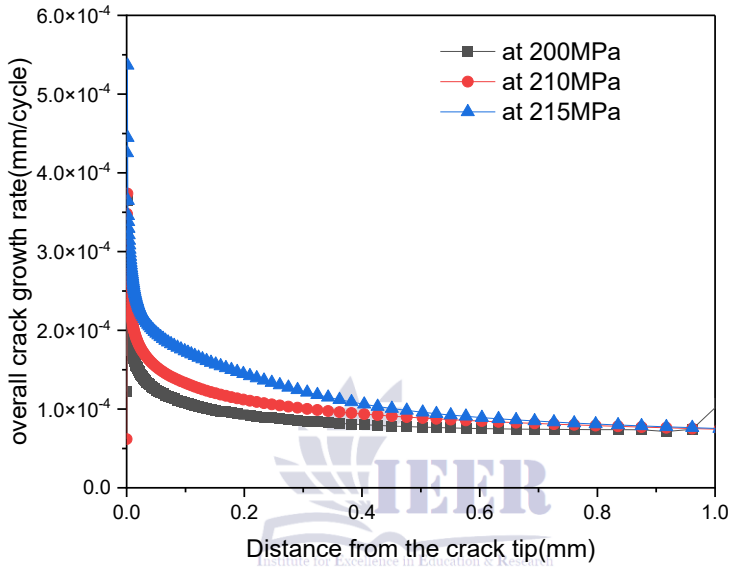

Figure 9. Overall crack growth rate vs. distance from crack tip

4. Conclusions

It can be concluded that the quantitative measurements of the SCC are affected by the presence of the low cyclic fatigue and time-integration framework models generates the better results of the overall crack growth rate as compared to the linear superposition method.

REFERENCES

[1] H. Jackson, K. Nibur, C. S. Marchi, J. P.-C. science, and undefined 2012, "Hydrogen-assisted crack propagation in 304L/308L and 21Cr–6Ni–9Mn/308L austenitic stainless steel fusion welds," Elsevier.

[2] H. Eisazadeh, A. Achuthan, J. A. Goldak, and D. K. Aidun, "Effect of material properties and mechanical tensioning load on residual stress formation in GTA 304-A36 dissimilar weld," J. Mater. Process. Technol., vol. 222, pp. 344–355, Aug. 2015, doi: 10.1016/j.jmatprotec.2015.03.021.

[3] K. Sieradzki and R. C. Newman, "Stress-corrosion cracking," Journal of Physics and Chemistry of Solids, 1987, doi: 10.1016/0022-3697(87)90120-X.

[4] J. C. Newman, E. P. Phillips, and M. H. Swain, "Fatigue-life prediction methodology using small-crack theory," Int. J. Fatigue, 1999, doi: 10.1016/S0142-1123(98)00058-9.

[5] R. Branco et al., "Low-Cycle Fatigue Behaviour of AISI 18Ni300 Maraging Steel Produced by Selective Laser Melting," Metals 2018, Vol. 8, Page 32, vol. 8, no. 1, p. 32, Jan. 2018, doi: 10.3390/met8010032.

[6] P. A. Bathias Claude, "1.3 Test Systems," Fatigue of Materials and Structures - Fundamentals, 2010, Accessed: Feb. 17, 2026. [Online]. Available: https://www.scribd.com/document/962294098/Fatigue-of-Materials-and-Structures-1st-Edition-Claude-Bathias

[7] M. Bassurucu and K. Turk, "An experimental and statistical investigation on the fresh and hardened properties of HFR-SCC: the effect of micro fibre type and fibre hybridization," European Journal of Environmental and Civil Engineering, vol. 27, no. 1, pp. 263–287, Jan. 2023, doi: 10.1080/19648189.2022.2042396.

[8] G. N.-A. C. Proceedings and undefined 2010, "Combined Finite-and Boundary-Element Analysis of SCC Crack Growth," pubs.aip.org, 2010, doi: 10.1063/1.3452270.

[9] S. Lozano-Perez, J. Dohr, M. Meisnar, and K. Kruska, "SCC in PWRs: Learning from a Bottom-Up Approach," Metallurgical and Materials Transactions E, vol. 1, no. 2, pp. 194–210, Jun. 2014, doi: 10.1007/s40553-014-0020-y.

[10] B. N. L. T. W Crooker, Corrosion Fatigue: Mechanics, Metallurgy, Electrochemistry, and Engineering, a Symposium. 1983.

[11] W. B. Wang, H. Xue, F. Q. Yang, and X. S. Zhou, "Characteristic of Interface Crack Propagation in Dissimilar Weld Joints," Adv. Mat. Res., vol. 988, pp. 249–252, 2014, doi: 10.4028/WWW.SCIENTIFIC.NET/AMR.988.249.

[12] T. Chu, C. Shao, Y. Wang, N. Ma, F. L.-M. & Design, and undefined 2022, "Crack branching behavior and amorphous film formation mechanism during SCC expanding test for multi-layers weld metal of NiCrMoV steels," Elsevier, Accessed: Feb. 12, 2026. [Online]. Available: https://www.sciencedirect.com/science/article/pii/S0264127522001411

[13] Y. Zhang, M. Zhang, and G. Ye, "Influence of moisture condition on chloride diffusion in partially saturated ordinary Portland cement mortar," Springer, vol. 51, no. 2, Apr. 2018, doi: 10.1617/s11527-018-1162-7.

[14] Z. Shen, ... S. L.-P. the 18th I. C. on, and undefined 2017, "A mechanistic study of the effect of temperature on crack propagation in alloy 600 under pwr primary water conditions," Springer, pp. 439–454, 2019, doi: 10.1007/978-3-030-04639-2_28.

[15] ELBER W, "FATIGUE CRACK CLOSURE UNDER CYCLIC TENSION," Eng. Fract. Mech., vol. 2, no. 1, pp. 37–44, 1970, doi: 10.1016/0013-7944(70)90028-7.

[16] P. Paris and F. Erdogan, "A critical analysis of crack propagation laws," Journal of Fluids Engineering, Transactions of the ASME, vol. 85, no. 4, pp. 528–533, 1963, doi: 10.1115/1.3656900.

[17] T. Kebir, J. Correia, ... M. B.-F. of A., and undefined 2021, "A FCG Model and the Graphical User Interface Under Matlab for Predicting Fatigue Life: Parametric Studies," bibliotekanauki.plT Kebir, JAFO Correia, M Benguediab, A ImadFatigue of Aircraft Structures, 2021•bibliotekanauki.pl, Accessed: Feb. 17, 2026. [Online]. Available: https://bibliotekanauki.pl/articles/2105193.pdf

[18] T. Ishihara, W. Maeng, S. Ohashi, ... Y. K.-J. of N., and undefined 1999, "Synergistic interaction of fatigue and stress corrosion on the corrosion fatigue crack growth behavior in Alloy 600 in high temperature and high pressure water," cir.nii.ac.jp, Accessed: Feb. 17, 2026. [Online]. Available: https://cir.nii.ac.jp/crid/1873116918018909952

[19] S. Mohanty, S. Majumdar, and K. Natesan, "A Review of Stress Corrosion Cracking/Fatigue Modeling for Light Water Reactor Cooling System Components," 2012.

[20] M. Knop, J. Heath, Z. Sterjovski, S. L.-P. Engineering, and undefined 2010, "Effects of cycle frequency on corrosion-fatigue crack growth in cathodically protected high-strength steels," ElsevierM Knop, J Heath, Z Sterjovski, SP LynchProcedia Engineering, 2010 • Elsevier, Accessed: Feb. 17, 2026. [Online]. Available: https://www.sciencedirect.com/science/article/pii/S1877705810001360

[21] R. Bashir, H. Xue, R. Guo, Y. Bi, and M. Usman, "Interaction of Cyclic Loading (Low-Cyclic Fatigue) with Stress Corrosion Cracking (SCC) Growth Rate," Advances in Materials Science and Engineering, vol. 2020, 2020, doi: 10.1155/2020/8026372.

[22] Y. Huang, F. Yang, N. Wang, ... M. Z. M., and undefined 2023, "Improvement of stress corrosion cracking resistance by low cycle fatigue of a CrNiMoV steel," nature.comYH Huang, FX Yang, N Wang, ML Zhu, FZ Xuannpj Materials Degradation, 2023 • nature.com, Accessed: Feb. 17, 2026. [Online]. Available: https://www.nature.com/articles/s41529-023-00372-3

[23] W. Zhang, H. Wu, S. Wang, Y. Hu, K. Fang, and X. Wang, "Investigation of Stress Corrosion Cracking Initiation in Machined 304 Austenitic Stainless Steel in Magnesium Chloride Environment," J. Mater. Eng. Perform., vol. 29, no. 1, 2020, doi: 10.1007/s11665-020-04558-7.

[24] A. Vainionpää, T. Seppänen, and Z. Que, "Effects of pressurized water reactor environment and cyclic loading parameters on the low cycle fatigue behavior of 304L stainless steel," Int. J. Fatigue, vol. 182, May 2024, doi: 10.1016/j.ijfatigue.2024.108231.

[25] R. Bashir, H. Xue, R. Guo, Y. Bi, and M. Usman, "Interaction of Cyclic Loading (Low-Cyclic Fatigue) with Stress Corrosion Cracking (SCC) Growth Rate," Wiley Online Library, vol. 2020, 2020, doi: 10.1155/2020/8026372.